

The mechanism of heat transfer in transition boiling

CHIN PAN, J. Y. HWANG and T. L. LIN

Department of Nuclear Engineering, National Tsing Hua University,
Hsinchu, Taiwan 30043, R.O.C.

(Received 9 May 1988 and in final form 29 November 1988)

Abstract—Liquid–solid contact in transition boiling is modelled by involving transient conduction, boiling incipience, macrolayer evaporation and vapour film boiling. The prediction of liquid contact duration and time fraction agrees reasonably well with experimental data, and the model is able to predict both of the boiling curve transitions—the critical and minimum heat fluxes. The study concludes that the liquid turbulence due to buoyancy forces and bubble agitation is an important parameter for transition boiling. It is found that surface coating (oxidation or deposition) tends to improve the transition boiling heat transfer and elevate the wall superheats at both the critical heat flux and the minimum film boiling points, which agree with the experimental observations.

1. INTRODUCTION

TRANSITION BOILING, which involves several unique features, including liquid–solid contacts, existence of at least two boiling curves and strong surface effects, is probably the least known regime of boiling heat transfer. Theoretical modelling of transition boiling is of interest in academic research and is of importance to industrial applications, such as nuclear reactor safety, quenching in material processing, etc.

It is now generally believed that liquid–solid contacts exist and result in large surface temperature oscillations in transition boiling [1]. Most of the energy diffused from the heating surface is probably transferred to the coolant at the instant of contact. However, it is not clear what kind of heat transfer mechanism is involved during contact.

The existence of two boiling curves in the transition boiling regime [2] is another peculiar feature, and again is not well understood. Experimentally it was found that, at the same wall superheat, the surface heat flux is higher during the heating process than during the cooling process. The difference between the two processes is found to be a strong function of surface wettability. Surfaces of good wetting show smaller differences, while surfaces of poor wetting present large deviations [3].

A significant surface effect is also a special feature of transition boiling. Berenson [4] first observed a significant surface effect on the transition boiling curve and indirectly demonstrated the existence of liquid–solid contacts. Early photographic studies [5, 6] did not support liquid–solid contact in this regime. Recently, the effects of surface roughness and wettability on transition boiling were systematically studied by Roy Chowdhury and Winterton [7]. They concluded that surface roughness does not play an important role, but that wettability significantly

affects transition boiling. However, other studies by Bui and Dhir [8] indicate that surface roughness may have a significant effect on, and surface oxidation or surface deposition may improve, transition boiling heat transfer. They explained the improvement by the increase in surface wettability. However, surface oxidation or surface deposition normally has poorer thermal conductivity than the original surface material. Since transient conduction plays an important role in liquid–solid contact, a layer of material of poor thermal properties on the surface may influence heat transfer in transition boiling significantly. In fact, it has been reported elsewhere [9] that a thin insulating layer on a heat transfer surface can elevate the minimum film boiling temperature and therefore improve the quenching process.

There are only limited theoretical studies analysing possible heat transfer mechanisms in transition boiling, although there are many published experimental investigations, in which much scattering of data was observed. These past modelling efforts are reviewed below. Many correlations have been proposed in the literature. However, very few of them give satisfactory predictions, owing to a lack of physical basis. There is therefore a need for sound theoretical study of transition boiling.

1.1. Past modelling efforts under pool boiling conditions

Bankoff and Mehra [10] proposed that transient conduction is the principal heat transfer mechanism during contact. This model seems to fail to explain the termination of contact.

Katto and Yokoya [11] proposed that boiling heat transfer at high heat fluxes is the dominant heat transfer mechanism during contact. At high heat fluxes, boiling heat transfer is characterized by the existence of a liquid film between the heating surface and by

NOMENCLATURE

b_1	$(k\rho C_p)_c^{1/2}/(k\rho C_p)_h^{1/2}$	t_v	time interval of vapour covering period [s]
b_2	$(k\rho C_p)_c^{1/2}/(k\rho C_p)_h^{1/2}$	u'_c	characteristic velocity [m s^{-1}]
C	constant coefficient in effective liquid thermal conductivity	v_{ig}	specific volume difference between saturated vapour and liquid [$\text{m}^3 \text{kg}^{-1}$]
C_p	specific heat at constant pressure [$\text{J kg}^{-1} \text{K}^{-1}$]	v_l	average volumetric growth rate of bubble [$\text{m}^3 \text{s}^{-1}$].
C_{sf}	constant coefficient of Rohsenow correlation		
F_A	instantaneous liquid contact-area fraction	Greek symbols	
F_θ	local liquid contact-time fraction	α	thermal diffusivity [$\text{m}^2 \text{s}^{-1}$]
g	gravitational constant [m s^{-2}]	β	thermal expansion coefficient [K^{-1}]
H_{ig}	latent heat of evaporation [J kg^{-1}]	δ_{me}	macrolayer thickness [m]
k	thermal conductivity [$\text{W m}^{-1} \text{K}^{-1}$]	Δ	coating thickness [m]
L	characteristic length scale [m]	λ_D	most dangerous Taylor wavelength [m]
l	eddy mixing length scale [m]	μ	viscosity [N s m^{-2}]
Pr	Prandtl number	ν	kinematic viscosity [$\text{m}^2 \text{s}^{-1}$]
q''	total heat flux [W m^{-2}]	ρ	density [kg m^{-3}]
q''_{cd}	heat flux during transient conduction [W m^{-2}]	σ	surface tension [N m^{-1}]
q''_{me}	heat flux during macrolayer evaporation [W m^{-2}]	τ	bubble hovering period [s].
q''_{nb}	nucleate boiling heat flux based on the surface temperature at the end of transient conduction [W m^{-2}]	Subscripts	
q''_v	vapour film boiling heat flux [W m^{-2}]	b	bulk liquid
R_d	bubble departure radius [m]	c	coating
r_c	surface cavity radius [m]	cd	transient conduction
T	temperature [K]	h	heater
T_b	bulk liquid temperature [K]	I	interface
ΔT_{sat}	surface (wall) superheat [K]	l	liquid
t_{cd}	time interval of transient conduction [s]	me	macrolayer evaporation
t_l	time interval of liquid contact [s]	nb	nucleate boiling
t_{me}	time interval of macrolayer evaporation [s]	sat	saturation
		t	turbulent property
		v	vapour
		w	wall or surface.

large mushroom-like bubbles [12, 13]. The bubble is nourished with vapour from many vapour stems which bridge the surface with the bubble. In the nucleate boiling regime, the film does not dry out. When critical heat flux is reached, the film evaporates away just at the time when the bubble leaves. In the transition boiling regime, the film evaporates away while the massive vapour bubble still hovers, and the surface remains dry for a period of time. Katto and Yokoya [11] assumed that the bubble period remains at that of the critical heat flux and that the nucleate boiling curve can be extrapolated into the transition boiling regime. Consequently, they were able to predict the film thickness and effective heat flux at a given surface temperature. The major difficulty of this model is that the surface temperature drop during the contact period was not considered. The nucleate boiling heat flux is a power-law function of wall superheat with an order of about 3 or more. Its evaluation based on the surface temperature before contact may be in serious error.

Kostyuk *et al.* [14] proposed a semi-empirical model for transition boiling. The model involves transient conduction, boiling incipience and heat transfer during liquid–solid contact. The termination of contact is caused by the coalescence of bubbles as they reach a critical population. Based on their own surface temperature measurements, a semi-empirical correlation with several empirical constants was reported. The correlation shows that the duration of liquid–solid contact falls very rapidly with a power of -4 of wall superheat in the low wall superheat range and falls slowly with a power of -2 in the high wall superheat range.

Recently, Farmer *et al.* [15, 16] developed a model for liquid–solid contact in the transition and film boiling regimes. The model is similar to that of Kostyuk *et al.* [14], and the contact is modelled by incorporating transient conduction, boiling incipience and heat transfer, and microlayer evaporation. The microlayer is the liquid film left below a fast growing bubble. When the number of bubbles formed per unit area is

large enough, the bubbles will coalesce, and subsequently force the bulk liquid to retreat and leave the liquid film below the bubble. The microlayer thus formed is quite thin. The model employs an accommodation coefficient for microlayer evaporation. In order to obtain a good fit with the data of Lee *et al.* [1], the accommodation coefficient was adjusted by as much as two orders of magnitude. However, no physical basis for this adjustment was given. In addition, the temperature oscillation predicted by the model is of the order of 10°C , which is much smaller than the measurements of Lee *et al.* [1].

In addition to the theoretical or semi-theoretical models discussed above, Hsu and Kim [17] recently proposed a statistical approach to treat transition boiling. The transition boiling curve is simulated by a Poisson distribution model. Given the location of a maximum or minimum point, the model can basically handle the surface effect, with the exception of surfaces having very large or very small contact angles.

1.2. Present study

In this investigation, a theoretical study of transition boiling under pool boiling conditions is conducted. Based on the experimental observation of temperature fluctuation in the literature, it is believed that the contact will involve the following mechanisms: transient conduction, boiling incipience and heat transfer, and formation and evaporation of the macrolayer. The major improvements of the current model include the following: (a) effects of surface coating (oxidation or deposition) and the inherently turbulent features of the contacting coolant are taken into account; (b) boiling heat transfer is considered to be at the high heat flux region, which is characterized by the formation of vapour jets rather than discrete bubbles at lower heat fluxes; (c) the bulk coolant is displaced owing to the Helmholtz instability, and a liquid film, referred to as the macrolayer, is left on the surface; (d) the boiling heat flux and thus the macrolayer thickness are determined on the basis of the temperature at the end of transient conduction, which is much lower than the temperature before contact. The model treats the two transitions in the boiling curve—the critical (maximum) and minimum heat fluxes—as natural translations from transition boiling to nucleate boiling and to film boiling, respectively. Both transitions are therefore predictable.

2. MODEL

The liquid–solid contact is modelled as shown in Fig. 1. As the bubble, which is sitting on the vapour film, leaves, bulk liquid will replace it and will tend to contact with the surface because of its inertia (Fig. 1(a)). As the contact takes place, the transient conduction period is started (Fig. 1(b)). The contacting liquid will be heated and a thermal boundary layer will be established by the energy diffusing from the heater through the surface coating or deposit if any.

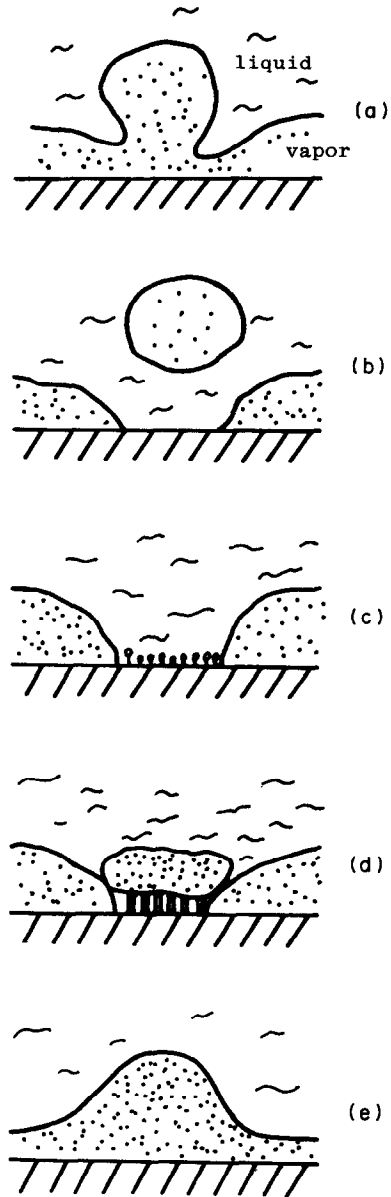


FIG. 1. Liquid–solid contact model: (a) bubble departing; (b) transient conduction; (c) boiling incipience and heat transfer; (d) macrolayer evaporation; (e) vapour covering.

Transient conduction is ended when boiling begins as incipient conditions are satisfied (Fig. 1(c)). As will be seen later, this boiling heat flux is relatively high. It can therefore be expected that the boiling is in a form of vapour jets similar to those seen in the high flux region, rather than discrete bubbles at low heat fluxes. The relative motion between vapour and liquid causes Helmholtz instability, and a massive bubble is formed as in the model of Haramura and Katto [18]. The bulk liquid then retreats (Fig. 1(d)). However, a liquid film, which is called a macrolayer, is left on the surface. This starts the macrolayer evaporation (boiling) period. The idea of macrolayer evaporation and the

associated vapour bubble hovering is an extension and modification of Haramura and Katto's critical heat flux model [18] to the transition boiling regime. Several new notions have been added in the present model, as will be explained in the following subsections. As the macrolayer evaporates, a bubble will be formed at the vapour-liquid interface (Fig. 1(e)). The liquid-solid contact is terminated by the evaporation of the macrolayer. This begins the vapour covering period. The bubble will continue to grow with vapour supplied by evaporation at the vapour-liquid interface. For pool boiling cases, since the bubble does not come into contact with the surface, the bubble departure is determined by the balance between the buoyancy force and the upward mass acceleration of the two-phase fluid [18]. A new liquid-solid contact begins as the bubble leaves. The detailed mechanism of each period is discussed below.

It should be noted that the liquid would probably come into intermittent contact with the solid at every point on the surface. The present model considers a representative contact cycle at any given point on the surface.

2.1. Transient conduction

Transient conduction begins at the moment that the liquid replaces the departing bubble and contacts the surface. In many cases, the heater surface may be coated with a thin film for experimental purposes [1, 19], oxidized with a thin oxide layer, or overlaid with a surface deposit of corrosion products by nature [8]. It has been well recognized that the presence of surface coating, oxidation or deposition significantly affects transition boiling by modifying the surface condition. However, surface coatings, oxidation or depositions generally have much poorer thermal properties than the heater. This can have a significant effect on transition boiling, so it is considered in this paper.

The transient conduction of the contacting liquid with the surface overlaid with a thin layer is analysed using a one-dimensional model. Details of this model are given in another paper [20]. The temperature at the interface of the liquid and solid is given as

$$T_i = T_b + \frac{T_w - T_b}{(1+b_1)(1+b_2)} \left\{ b_2(1+b_1) \times \sum_{n=0}^{\infty} \left[\frac{(1-b_1)(1-b_2)}{(1+b_1)(1+b_2)} \right]^n \operatorname{erfc} \left(\frac{n\Delta}{\sqrt{\alpha_c t}} \right) + b_2(1-b_1) \times \sum_{n=0}^{\infty} \left[\frac{(1-b_1)(1-b_2)}{(1+b_1)(1+b_2)} \right]^n \operatorname{erfc} \left[\frac{(n+1)\Delta}{\sqrt{\alpha_c t}} \right] \right\} \quad (1a)$$

$$b_1 = (k\rho C_p)_c^{1/2} / (k\rho C_p)_h^{1/2} \quad (1b)$$

$$b_2 = (k\rho C_p)_c^{1/2} / (k\rho C_p)_h^{1/2}. \quad (1c)$$

From equation (1a), one can see that the interface temperature is a function of the temperature difference between the surface and the bulk liquid before contact

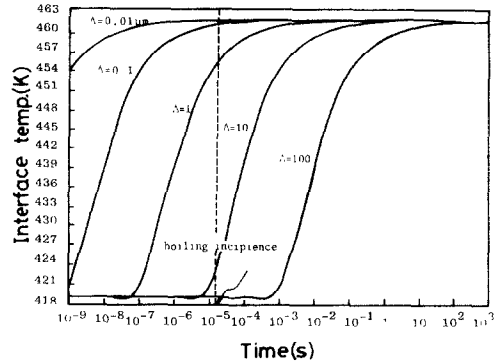


FIG. 2. Interfacial temperature as a function of time and layer thickness. The surface is copper overlaid with Al_2O_3 . The effective thermal conductivity of water is assumed to be $60 \text{ W m}^{-1} \text{ K}^{-1}$.

and the thermal properties of liquid, thin layer and heater material. In addition, it is a function of time, which is in contrast to the case of transient contact of two semi-infinite bodies. For the later case, the interface temperature is independent of time.

It can be shown [20] that the interface temperature behaves like the transient contact of liquid and coating only as the coating thickness approaches infinity or at the early stage of contact. Thus, equation (1a) becomes the following well-known equation by letting Δ approach infinity or t approach 0:

$$T_i = T_b + (T_w - T_b) \frac{(k\rho C_p)_c^{1/2} / (k\rho C_p)_h^{1/2}}{1 + (k\rho C_p)_c^{1/2} / (k\rho C_p)_h^{1/2}}, \quad \Delta \rightarrow \infty \text{ or } t \rightarrow 0. \quad (1d)$$

In contrast, it can also be shown [20] that the interface temperature behaves like transient contact of liquid and heater only as the coating thickness approaches zero or at the later stage of contact. Under one or both of these two conditions, equation (1a) becomes

$$T_i = T_b + \frac{(T_w - T_b)}{(1+b_1)(1+b_2)} 2b_2 \times \sum_{n=0}^{\infty} \left[\frac{(1-b_1)(1-b_2)}{(1+b_1)(1+b_2)} \right]^n. \quad (1e)$$

By equating the liquid and coating temperatures at the interface, it can be shown that [20]

$$\sum_{n=0}^{\infty} \left[\frac{(1-b_1)(1-b_2)}{(1+b_1)(1+b_2)} \right]^n = \frac{(1+b_1)(1+b_2)}{2(b_1+b_2)}. \quad (1f)$$

Substituting equation (1f) into equation (1e) yields

$$T_i = T_b + (T_w - T_b) \frac{(k\rho C_p)_h^{1/2} / (k\rho C_p)_c^{1/2}}{1 + (k\rho C_p)_h^{1/2} / (k\rho C_p)_c^{1/2}}, \quad \Delta \rightarrow 0 \text{ or } t \rightarrow 0. \quad (1g)$$

This agrees with the result for a zero coating thickness.

Figure 2 shows the interface temperature of water in contact with a copper heater overlaid with a thin layer of Al_2O_3 as a function of time and layer thick-

ness. For this case, the layer material has much poorer thermal properties than the heater. The interface temperature changes rapidly from a constant low value to a constant high value. The actual temperature drop due to the transient conduction is determined by the time at which boiling begins.

The thermal conductivity of the contacting liquid deserves special attention. The contacting liquid, which is from the region outside the departing bubble, is not a stagnant fluid but is characterized by internal circulation and turbulence. Lee *et al.* [1], using Bankoff and Mehra's model [10], have found that the boiling curve is bounded by assuming that the contacting liquid is stagnant or highly turbulent, respectively. Therefore, it is reasonable to assume that the effective thermal conductivity of contacting liquid includes a molecular term and a turbulent term, i.e.

$$k_{eff} = k_1 + k_t \tag{2}$$

For the pool boiling case, the turbulence within the liquid may result from the natural convection and bubble disturbance.

Using simple mixing theory, the turbulent diffusivity of the liquid can be given as

$$\alpha_t \approx v_t \approx \mu'_c l \tag{3}$$

where μ'_c is a characteristic velocity associated with the turbulent velocity fluctuations and l is a characteristic mixing length.

In transition boiling, the temperature head is large. It would be expected that the natural convection due to this temperature head dominates the velocity scale. Consequently, it is reasonable to assume that in the region sufficiently far away from the surface the liquid acceleration is caused by the buoyancy force. Thus, the characteristic velocity scale is given as

$$u'_c \propto \sqrt{[g\beta(T_w - T_b)]L} \tag{4}$$

The possible effects of bubble agitation on the velocity scale are embedded in the characteristic length scale, L . For boiling heat transfer, it is reasonable to assume that the bubble departure diameter is the characteristic length and turbulent mixing length scales. Thus

$$l \propto R_d \tag{5a}$$

and

$$L \propto R_d \tag{5b}$$

The bubble departure radius in transition boiling, as in film boiling, is governed by Taylor instability [21] and is proportional to $[\sigma/g(\rho_1 - \rho_v)]^{1/2}$ (see equation (14)). To account for the possible wall temperature influence, the bubble departure radius may be related to the surface temperature and temperature head as follows [15, 16]:

$$R_d \propto \left[\frac{\sigma}{g(\rho_1 - \rho_v)} \right]^{1/2} \frac{(T_w - T_b)}{T_w} \tag{6}$$

Combining equations (3)–(6) leads to

$$\alpha_t = C(g\beta)^{1/2} \left[\frac{\sigma}{g(\rho_1 - \rho_v)} \right]^{3/4} \frac{(T_w - T_b)^2}{(T_w)^{3/2}} \tag{7}$$

The only unknown in equation (7) is the coefficient C , which can be determined by comparing equation (7) with experimental measurements of liquid contact duration, as will be done in the following section.

Transient conduction ends when boiling begins. The time interval between the start of transient conduction and incipient boiling is called the transient conduction period, t_{cd} .

2.2. Boiling incipience and heat transfer

As the liquid thermal boundary is establishing, boiling can be predicted by the model of Hsu [22]. The model requires that for boiling incipience the liquid temperature at the bubble tip be greater than or equal to the vapour temperature

$$T_1(x = r_c, t) \geq T_g = T_{sat} + \frac{2\sigma T_{sat} v_{fg}}{r_c H_{fg}} \tag{8a}$$

Using equation (8a) and the liquid temperature distribution [20]

$$\begin{aligned} T_1(x, t) = & T_b + \frac{T_w - T_b}{(1 + b_1)(1 + b_2)} \left\{ b_2(1 + b_1) \right. \\ & \times \sum_{n=0}^{\infty} \left[\frac{(1 - b_1)(1 - b_2)}{(1 + b_1)(1 + b_2)} \right]^n \operatorname{erfc} \left(\frac{x}{2\sqrt{(\alpha_c t)}} + \frac{n\Delta}{\sqrt{(\alpha_c t)}} \right) \\ & + b_2(1 - b_1) \sum_{n=0}^{\infty} \left[\frac{(1 - b_1)(1 - b_2)}{(1 + b_1)(1 + b_2)} \right]^n \\ & \left. \times \operatorname{erfc} \left(\frac{x}{2\sqrt{(\alpha_c t)}} + \frac{(n + 1)\Delta}{\sqrt{(\alpha_c t)}} \right) \right\} \tag{8b} \end{aligned}$$

the time for the end of transient conduction and boiling incipience can be predicted for a given surface condition (cavity size distribution). On the other hand, an optimal cavity size, which gives the shortest time for boiling incipience, can be determined.

The boiling heat flux corresponding to the surface superheat at the end of transient conduction can be evaluated by an appropriate correlation. In this study, the well-known correlation by Rohsenow is employed

$$\frac{C_p [T_1(t = t_{cd}) - T_{sat}]}{H_{fg} Pr^{1.7}} = C_{sf} \left[\frac{q'_{nb}}{\mu H_{fg}} \sqrt{\left(\frac{\sigma}{g(\rho_1 - \rho_v)} \right)} \right]^{0.33} \tag{9}$$

In equation (9), the value of C_{sf} is a function of liquid–surface combination; a value of 0.013 is used in this study. An exponent of 1.7 on the Prandtl number, as Rohsenow originally suggested, has been used in this

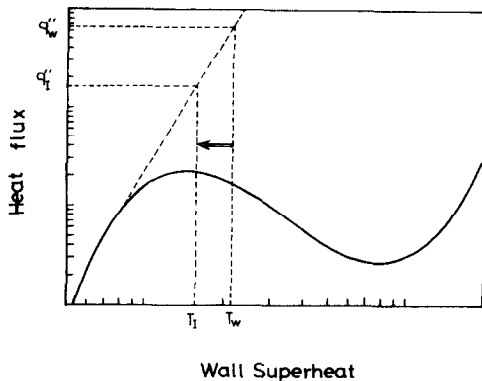


FIG. 3. Significant difference in boiling heat fluxes based on surface temperatures before and after transient conduction, respectively.

study. Later, Rohsenow recommended an exponent of 1.0 for water only.

It is possible that the adoption of the Rohsenow correlation under the present rapid transient conditions and high heat flux conditions may introduce a certain uncertainty, as the correlation was developed for steady-state conditions and for heat fluxes below the critical heat flux. This uncertainty in conjunction with other possible uncertainties caused by the choice of the value of C_{sf} and the exponent of the Prandtl number may be absorbed by proper choice of the coefficient, C , for the effective thermal conductivity (see equation (7)), which requires the comparison of model predictions with experimental measurements of liquid contact duration as will be done in the following section.

Note that in equation (9), heat flux is evaluated on the basis of the surface temperature at the end of transient conduction, by which time the surface has been subject to a substantial temperature drop. Since the heat flux is very sensitive to the surface superheat, and this temperature drop could be as high as 125 K [1], the temperature drop in the conduction period plays a very important role in determining the boiling heat flux. In the literature, see, e.g. ref. [11], boiling heat flux is evaluated on the basis of the surface temperature before contact, which may cause serious errors, as shown in Fig. 3.

Although there is a substantial temperature drop due to transient conduction, the boiling heat flux thus evaluated is still quite high (generally near the critical heat flux). It is, therefore, reasonable to assume that boiling heat transfer is in terms of vapour jets rather than the discrete bubbles shown in Fig. 1. Moissis and Berenson [23] have derived a criterion to distinguish these two boiling regimes.

The time interval between bubble incipience and formation of vapour jets is relatively small compared with the liquid contact duration. The diameter of vapour jets ranges typically from 0.1 to 1 mm and decreases with increasing heat flux; for heat fluxes greater than 10^6 W m^{-2} , the data trend indicates that

the diameter could be less than 0.1 mm [12]. Since the wall superheat during transition boiling, even after the temperature drop during the transient conduction, is quite high and the vapour jet sizes are relatively small, it is reasonable to assume that bubble growth is inertia controlled and can be estimated by the Rayleigh equation. Assuming the bubble size at the incipient moment is $1 \mu\text{m}$, and assuming that 50 K of surface superheat results in a bubble growth time of 9×10^{-6} – 9×10^{-5} s, which is much smaller than the typical liquid contact duration time ranging from 10^{-3} to 10^{-2} s [1]. The time interval and the associated heat transfer between boiling incipience and formation of vapour jets are therefore neglected.

2.3. Macrolayer evaporation

It is proposed that the relative motion between vapour and liquid will cause Helmholtz instability and cause the bulk liquid to retreat from the surface. However, the presence of a surface may suppress the instability, and a liquid film called the 'macrolayer' will be left on the surface [18]. The film is referred to as a macrolayer to distinguish it from the microlayer below a fast growing bubble. This marks the end of boiling heat transfer and starts the macrolayer evaporation.

Haramura and Katto [18] argued that the macrolayer thickness is approximately equal to one quarter of the critical wavelength of Helmholtz instability, and derived the following equation for macrolayer thickness:

$$\frac{\delta_{mc}(q''/H_{fg})^2}{\sigma\rho_v} = 0.00536 \left(\frac{\rho_v}{\rho_l}\right)^{0.4} \left(1 + \frac{\rho_v}{\rho_l}\right). \quad (10a)$$

For the present study, q''_{nb} evaluated from equation (9) is used to determine the macrolayer thickness. Note that the macrolayer thickness is inversely proportional to the square of the heat flux.

There have been arguments about whether nucleate boiling exists on surfaces covered with a thin liquid film. However, experimental studies in transition boiling [14, 24] tend to support the existence of nucleate boiling. Small temperature fluctuations which indicate the occurrence of nucleate boiling have been observed after the surface temperature has been lowered by transient conduction. Yu and Mesler [25] have demonstrated that nucleate boiling takes place in a macrolayer.

Nucleate boiling in a thin liquid film is generally more efficient than in pool boiling [26]. However, there is lack of a generally acceptable correlation. In this study, it is assumed that the Rohsenow correlation, i.e. equation (9), can still be applied throughout the period of macrolayer evaporation. The uncertainty due to this assumption will be discussed further in Section 2.6. Thus

$$q''_{mc} = q''_{nb} \quad (10b)$$

and the time interval for the macrolayer to evaporate away is thus given as

$$t_{me} = \delta_{me} \rho_l H_{fg} / q''_{me}. \quad (11)$$

2.4. Vapour covering

The dryout of the macrolayer marks the end of liquid–solid contact and starts the vapour covering period. The evaporation of the macrolayer provides vapour for the bubble to grow at the interface of the vapour and bulk liquid. If the bubble has not left at the end of macrolayer evaporation, the bubble will continue to grow with vapour supplied from the evaporation at the interface of vapour and bulk liquid. Since the bubble is not sitting on the surface, the bubble departure is determined by the balance of buoyancy force and the upward mass acceleration of the two-phase fluid [27, 28]. The hovering time for a bubble of volumetric growth rate v_1 is given as [18]

$$\tau = \left(\frac{3}{4\pi}\right)^{1/5} \left[\frac{4 \left(\frac{11}{16} \rho_l + \rho_v \right)}{g(\rho_l - \rho_v)} \right]^{3/5} v_1^{1/5}. \quad (12)$$

The average volumetric growth rate of the bubble in the periods of macrolayer evaporation and vapour covering is given by

$$v_1 = \lambda_D^2 q''_{ave} / (\rho_v H_{fg}) \quad (13)$$

where λ_D is the most dangerous Taylor wavelength [29]

$$\lambda_D = 3^{1/2} 2\pi [\sigma / g(\rho_l - \rho_v)]^{1/2}. \quad (14)$$

In equation (14), it is assumed that the unit heater area participating in the growth of one vapour bubble is λ_D^2 .

The average heat flux within these two periods is given as

$$q''_{ave} = \frac{q''_{me} t_{me} + (\tau - t_{me}) q''_v}{\tau} \quad (15)$$

where q''_v is the heat flux during the vapour covering period and will be given later in equation (20). Combining equations (12)–(15) gives a transcendental equation for determining the bubble hovering time, τ . Once τ is determined, the vapour covering period can be determined as

$$t_v = \tau - t_{me}. \quad (16)$$

In equation (16), if $\tau < t_{me}$ there is no vapour covering period, since the bubble leaves before the macrolayer evaporates away. This is the situation for nucleate boiling. Consequently, the model is also able to predict nucleate boiling heat transfer near the critical heat flux. This requires the transition from transition boiling to nucleate boiling. The critical heat flux, which appears when $\tau = t_{me}$, is therefore also predictable. The idea that the critical heat flux appears when the liquid film evaporates away at the end of the

vapour bubble hovering period was first postulated by Haramura and Katto [18].

2.5. Time fraction vs area fraction

The time fraction of liquid–solid contact is given as

$$F_\theta = \frac{t_l}{t_l + t_v}. \quad (17)$$

The liquid contact duration consists of three parts: transient conduction, boiling heat transfer and macrolayer evaporation. Thus

$$t_l = t_{cd} + t_{nb} + t_{me} \cong t_{cd} + t_{me}. \quad (18)$$

Assuming that the contact is an ergodic process, the following equality can be applied:

$$F_\theta = F_A \quad (19)$$

where F_A is the area fraction of liquid–solid contact. The criteria for meaningful measurements of F_θ and F_A are given by Lee *et al.* [1].

2.6. Transition boiling curve

To find the heat flux at a certain value of wall superheat before contact is the essential part of transition boiling studies. On the basis of the model presented in the previous subsections, the heat flux includes three contributions—transient conduction, macrolayer evaporation and vapour film boiling. The weighting of these three contributions is determined by their contact-time fraction as follows:

$$q'' = \frac{q''_{cd} t_{cd} + q''_{me} t_{me} + q''_v t_v}{t_{cd} + t_{me} + t_v}. \quad (20)$$

Equation (20) can be written as

$$q'' = \bar{q}''_{cd} + \bar{q}''_{me} + \bar{q}''_v \quad (21a)$$

$$\bar{q}''_{cd} = q''_{cd} t_{cd} / (t_{cd} + t_{me} + t_v) \quad (21b)$$

$$\bar{q}''_{me} = q''_{me} t_{me} / (t_{cd} + t_{me} + t_v) \quad (21c)$$

$$\bar{q}''_v = q''_v t_v / (t_{cd} + t_{me} + t_v). \quad (21d)$$

The uncertainty of assuming that the macrolayer evaporation heat flux (q''_{me}) equals the nucleate boiling heat flux (q''_{nb}) from the Rohsenow correlation on the transition boiling heat flux may be examined by equation (21c). Equation (11) indicates that the numerator of equation (21c) is independent of q''_{me} . On the other hand, the major components of the denominator are t_{me} and t_v . As can be seen from equation (11), t_{me} is inversely proportional to q''_{me} . On the other hand, t_v increases slowly with increasing q''_{me} as suggested by equations (12)–(16). Consequently, at the upper part of the transition boiling curve, where t_{me} and t_v have the same order of magnitude, the assumption that $q''_{me} = q''_{nb}$ may somewhat underestimate the transition boiling heat flux, in that boiling in a thin liquid film is more efficient than pool boiling. At the lower part of the transition boiling curve, where t_v is much greater than t_{me} , the transition boiling heat flux is insensitive to the uncertainty in q''_{me} .

The transient conduction makes heat flux a strong function of time [20]

$$\begin{aligned}
 q''_{cd}(t) &= (T_w - T_b) \frac{b_2}{(1+b_2)} \frac{k_1}{\sqrt{(\pi\alpha_1 t)}} \\
 &+ (T_w - T_b) \frac{b_2}{(1+b_2)} \sum_{n=1}^{\infty} \left[\frac{(1-b_1)(1-b_2)}{(1+b_1)(1+b_2)} \right]^n \\
 &\times \exp\left(-\frac{n^2\Delta^2}{\alpha_c t}\right) + (T_w - T_b) \frac{b_2(1-b_1)}{(1+b_1)(1+b_2)} \\
 &\times \sum_{n=0}^{\infty} \left[\frac{(1-b_1)(1-b_2)}{(1+b_1)(1+b_2)} \right]^n \exp\left(-\frac{(n+1)^2\Delta^2}{\alpha_c t}\right).
 \end{aligned} \tag{22}$$

In equation (20), a value of $q''_{cd}(t)$ averaged over the period of t_{cd} is used

$$\begin{aligned}
 \bar{q}''_{cd} &= \frac{k_1}{\sqrt{(\pi\alpha_1 t_{cd})}} (T_w - T_b) \frac{2b_2}{(1+b_2)} \\
 &+ \frac{k_1}{\sqrt{(\pi\alpha_1 t_{cd})}} (T_w - T_b) \frac{b_2}{(1+b_2)} \\
 &\times \sum_{n=1}^{\infty} \left\{ \left[\frac{(1-b_1)(1-b_2)}{(1+b_1)(1+b_2)} \right]^n M(a_n) \right\} + \frac{k_1}{\sqrt{(\pi\alpha_1 t_{cd})}} \\
 &\times (T_w - T_b) \frac{b_2(1-b_1)}{(1+b_1)(1+b_2)} \\
 &\times \sum_{n=0}^{\infty} \left\{ \left[\frac{(1-b_1)(1-b_2)}{(1+b_1)(1+b_2)} \right]^n M(a_{n+1}) \right\}
 \end{aligned} \tag{23a}$$

where

$$\begin{aligned}
 M(a_n) &= a_n^{-1} \exp(-a_n) \sum_{m=0}^{\infty} (-1)^m \\
 &\times \frac{1 \cdot 3 \cdot 5 \cdots (2m+1)}{2^m} a_n^{-m}, \quad \text{if } a_n \rightarrow \infty
 \end{aligned} \tag{23b}$$

$$M(a_n) = 2a_n^{1/2} [a_n^{-1/2} - \sqrt{\pi}], \quad \text{if } a_n \rightarrow 0 \tag{23c}$$

$$a_n = \frac{n^2\Delta^2}{\alpha_c t_{cd}}. \tag{23d}$$

The second and third terms in equation (23a), which are generally much smaller than the first term, are obtained by the asymptotic expansions of the integrals [30] of the second and third terms in equation (22). For more accurate results, numerical integrations have been applied in this study.

The heat flux during the vapour covering period is given by [15, 16]

$$q''_v = k_v \frac{\Delta T_{sat}}{\Delta_{film}}. \tag{24a}$$

The vapour film thickness, Δ_{film} , is given by [21]

$$\Delta_{film} = 2.35 \left[\frac{\mu_v k_v \Delta T_{sat}}{H_{fg} \rho_v g (\rho_l - \rho_v)} \sqrt{\left(\frac{\sigma}{g(\rho_l - \rho_v)} \right)} \right]^{1/4}. \tag{24b}$$

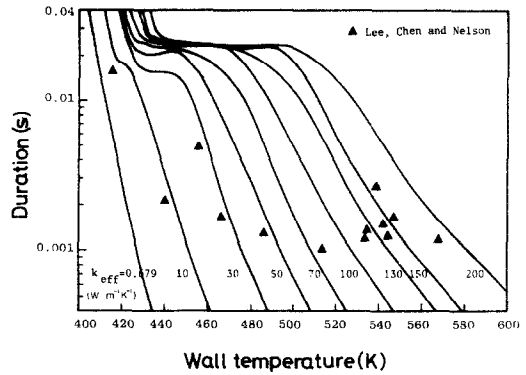


FIG. 4. Liquid contact duration as a function of liquid effective thermal conductivities and pre-contact wall temperature.

In equations (24a) and (24b), for simplicity, ΔT_{sat} is assumed to be the wall superheat at the end of the macrolayer evaporation period. The vapour properties are evaluated at $T_w - \Delta T_{sat}/2$. ΔT_{sat} is determined by solving a transient one-dimensional heat conduction problem in the coating and heater regions. The initial condition is the temperature distribution at the end of the transient conduction period. The boundary condition at the coating surface is the heat flux given by the macrolayer evaporation [20].

It should be noted that equation (24b) is for a continuous vapour film, which is not exactly the same as that in transition boiling. It is adopted in this study because the heat transfer during the vapour covering period in transition boiling is only a minor contributor except at the region near the minimum film boiling point, at which the vapour film approaches the continuous one described by equation (24b).

3. MODEL EVALUATION AND DISCUSSIONS

The model presented in the last section is evaluated in this section. The evaluation is primarily based on a reference case that simulates the experimental conditions of Lee *et al.* [1], which are given as follows: coolant is saturated water at atmospheric pressure, and the heater is copper overlaid with a thin layer of aluminium oxide (Al_2O_3) 16 μm thick. The oxide was due to the oxidation of aluminium, which was used as a junction for the fast-response surface microthermocouple. The oxidation resulted from the fact that the experiments were conducted in open air [1]. The surface is assumed to have cavities of size of 1 μm . The sensitivity of this assumption will be examined later.

3.1. Effective liquid thermal conductivity

The determination of the effective liquid thermal conductivity requires the evaluation of the coefficient in equation (7). Figure 4 shows the comparison of model predictions using k_{eff} as the parameter and measurements of run No. 1 in Lee *et al.* [1] of contact

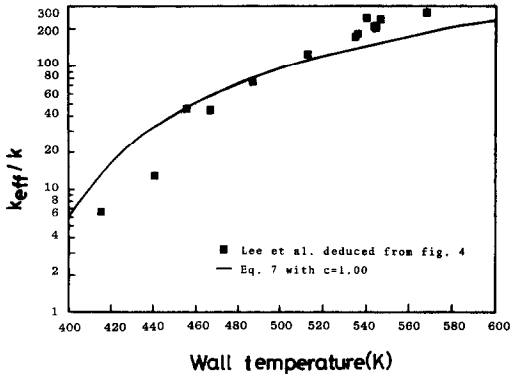


FIG. 5. Effective thermal conductivities as a function of pre-contact wall temperature.

duration as a function of the pre-contact wall temperature. The comparison indicates that a specific measurement at a given temperature is predictable if an appropriate k_{eff} is given. For example, at a wall temperature of 488 K, a k_{eff} of 48 $W m^{-1} K^{-1}$ results in a prediction of the duration in agreement with the result at this temperature of Lee *et al.* [1]. On the other hand, proper values of k_{eff} as a function of temperature can be determined if good agreement between model predictions and measurements is assumed. This gives a way to determine the best value of the coefficient in equation (7). Figure 5 shows the comparison of k_{eff} evaluated from equation (7) with $C = 1.00$ and those determined from Fig. 4. It is seen that agreement is fairly good and plausible. The turbulent model predicts the right trend of k_{eff} as a function of temperature. k_{eff} predicted from equation (7) with $C = 1.00$ is used for more model predictions in the following subsections.

3.2. Wall temperature drop after transient conduction

The surface temperature drop at the end of transient conduction is of great interest since it determines the boiling heat flux and therefore the macrolayer thickness and the evaporation heat flux. Figure 6 shows the surface temperature and temperature drop at the

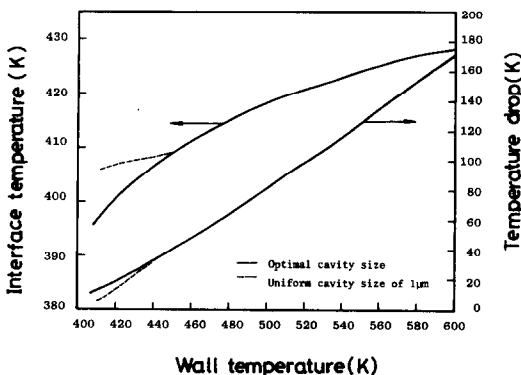


FIG. 6. Surface temperature and temperature drop at the end of transient conduction.

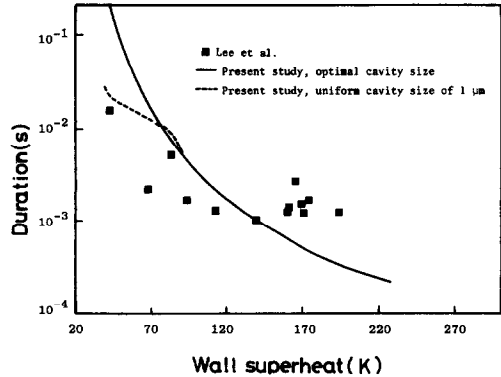


FIG. 7. Comparison of liquid contact duration between model prediction and experimental measurement.

end of transient conduction as a function of the pre-contact wall temperature. The two predictions are based on (a) a uniform cavity size of $1 \mu m$ and (b) the optimal cavity size, which gives the shortest time for the boiling incipience at a given pre-contact wall temperature and decreases—from about $3 \mu m$ to about $1 \mu m$ —with increasing pre-contact wall temperature. It can be seen that the two cavity sizes predict almost the same results except at the region of lower pre-contact wall temperatures, where nucleate boiling is predominant. The plot indicates that the temperature drop increases approximately linearly with increasing the pre-contact wall temperature. This linearity is supported by the measurements of Aoki and Welty [31]. The trend of increasing temperature drop with increasing wall superheat is also supported by the experiments of Lee *et al.* [1]. Their temperature history indicates that the temperature fluctuation increases with increasing wall superheat at lower wall superheats. At higher wall superheats, however, the fluctuation is not as high as at lower superheats. This may result from the thermocouple being unable to respond to the fast transient at higher wall superheats.

Figure 6 also shows that the temperature drop can be greater than 100 K at higher wall superheats. Lee *et al.* [1] have reported a temperature drop as high as 125 K, which supports the high temperature drop predicted by the present model. Previous models in the literature, e.g. refs. [15, 16], were not able to predict this high temperature drop.

The consistency of the linearity and high temperature drops between the model predictions and the measurements supports the existence of liquid turbulence.

3.3. Liquid contact duration and contact time fraction

The model predictions of liquid contact duration are compared with the data of Lee *et al.* [1] in Fig. 7. The two predictions are based on (a) a uniform cavity size of $1 \mu m$ and (b) the optimal cavity size. At medium and higher wall superheats, the two cavity sizes result in almost the same contact duration, while at lower wall superheats, the optimal cavity size gives longer

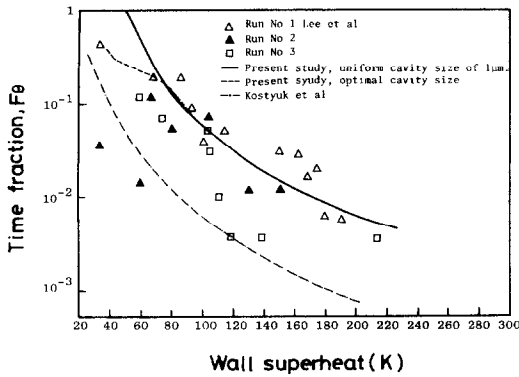


FIG. 8. Comparison of liquid contact-time fraction between model prediction and experimental measurement.

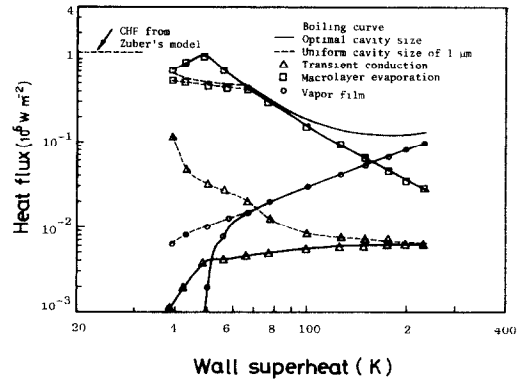


FIG. 9. Transition boiling curve for the reference case.

contact duration. Both the predictions and the measurements indicate that the duration generally decreases with increasing the pre-contact wall superheat. Agreement is satisfactory at lower wall superheats, while the predictions underestimate the duration at higher wall superheats, owing to underprediction of k_{eff} at high pre-contact wall temperatures, as shown in Fig. 5. It is worth noting that the major contributor to the liquid contact duration is the macrolayer evaporation period. The transient conduction period for this case lasts about 10^{-6} s, which is much shorter than the liquid duration time, which is of the order of 10^{-3} s, as shown in Fig. 7.

The liquid contact-time fraction is shown in Fig. 8 as a function of the pre-contact wall superheat. Considering the data scattering in the measurements of Lee *et al.* [1], the model predictions are quite satisfactory. As to the predictions of the liquid contact duration, at medium and higher wall superheats the predictions using the optimal cavity size are almost the same as those using a uniform cavity size of $1 \mu\text{m}$; at lower wall superheats, the latter predicts a lower liquid contact-time fraction. The current model predictions are much better than those by the semi-theoretical model of Kostyuk *et al.* [14], which always predicts the lower bound of the measurements (Fig. 8).

3.4. Transition boiling curve

The determination of the boiling curve is one of the major interests of transition boiling. Figure 9 shows the predicted transition boiling curve for the reference case using (a) the optimal cavity size and (b) a uniform cavity size of $1 \mu\text{m}$. No calculations for the case using a uniform cavity size of $1 \mu\text{m}$ were carried out since the wall superheat is lower than 38 K, below which temperature the thermal boundary layer established by the transient conduction would never reach the criterion for boiling incipience. It can be seen that using the optimal cavity size results in a higher transition boiling heat flux than using a uniform cavity size of $1 \mu\text{m}$. For a surface without a specific description of

surface characteristics, using the optimal cavity size is probably more reasonable.

The relative contributions to the boiling curve due to the transient conduction, macrolayer evaporation and vapour film boiling, respectively, are also presented in Fig. 9. The macrolayer evaporation is the major contributor of the three. The transient conduction does not transport a significant amount of heat flux, except at lower wall superheats for a surface with a uniform cavity size of $1 \mu\text{m}$. At lower wall superheats, as expected, the vapour film boiling is the smallest contributor. At higher wall superheats, vapour film boiling becomes increasing important, and it is dominant at very high wall superheats, in which transition boiling is translated into film boiling.

Using the optimal cavity size, both transitions in the pool boiling curve are predicted by the model. Figure 9 shows that the present model predicts not only the minimum film boiling point but also the critical heat flux, which agrees reasonably well with the value predicted by Zuber's hydrodynamic theory [32]. The minimum film boiling point predicted by the model is also reasonable.

Significant effects of surface coating on the transition boiling curve are presented in Fig. 10. Both curves are obtained using the optimal cavity size. For the non-coated (copper) surface, the optimal cavity size is smaller than for the coated surface. The figure

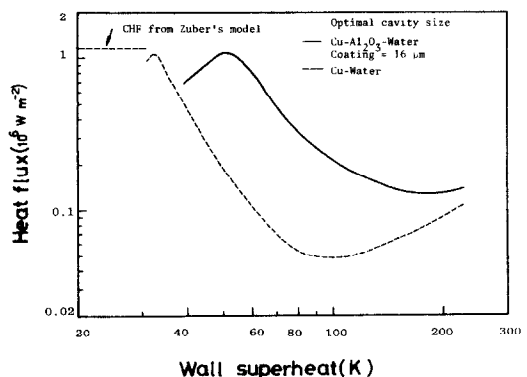


FIG. 10. Effect of insulating layer on transition boiling heat flux.

shows that the presence of an insulating layer (Al_2O_3) on the highly conducting surface (copper) dramatically increases the transition boiling heat flux. The presence of the insulating layer increases the surface temperature drop at the end of the transient conduction. Thus, a thicker macrolayer (see equations (9) and (10)) will result. Since macrolayer evaporation is the major contributor, a thicker macrolayer means a higher transition boiling heat flux. Similar effects due to surface oxidation or surface deposition have been observed experimentally [8]. The improvement in transition boiling was explained by the better wettability of the oxide or deposit. The present study indicates that the thermal properties of the surface coating are probably the major cause, or at least one of the reasons. The experiments conducted by Westwater and co-workers [33, 34] also show a significant effect of metal thermal properties on the boiling curves. A metal with very poor thermal properties, such as bismuth, present a significantly higher transition boiling heat flux than other metals with better thermal properties.

Figure 10 shows that the critical heat flux is only slightly increased by and is basically independent of the presence of an insulating layer. This agrees with Zuber's hydrodynamic model [32] which shows that the critical heat flux is independent of surface condition. However, recent experiments conducted in ref. [8] indicate that the critical heat flux is somewhat increased by a surface oxidation or deposition. This may be due to the surface wettability, which is not considered in the present model. Although the model predicts that the critical heat flux level is basically independent of the surface material, the wall superheat at the critical heat flux point is strongly surface material dependent. The presence of an Al_2O_3 layer ($16\ \mu\text{m}$) copper surface increases the wall superheat at the critical heat flux point. This prediction is also supported by the experiments conducted by Westwater and co-workers [33, 34], which show that the metals with poorer thermal properties present higher wall superheats at the critical heat flux point.

The presence of an insulating layer elevates the minimum film boiling temperature as shown in Fig. 10. The elevation of minimum film boiling temperature due to a thin insulating layer has also been reported in the literature [9]. Similarly, Westwater and co-workers [33, 34] observed that the wall superheat at the minimum film boiling point is higher for the metals with poorer thermal properties than for the metals with better thermal properties.

Figure 11 shows the comparison of model predictions and measurement of Dhuga and Winterton [19]. The model predictions are obtained using the optimal cavity size, which decreases—from about $3\ \mu\text{m}$ to about $1\ \mu\text{m}$ —with increasing wall superheat. The heating surface used by Dhuga and Winterton was of aluminium anodized with a barrier film of non-porous Al_2O_3 . The thickness of the barrier is

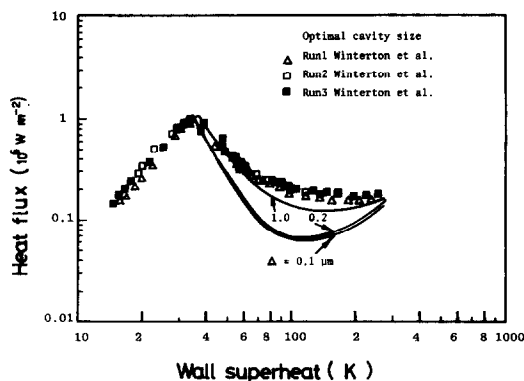


FIG. 11. Comparison of transition boiling curve between model prediction and data of Dhuga and Winterton [19]. The oxide layer is $0.1\text{--}0.2\ \mu\text{m}$ thick.

estimated to be $0.1\text{--}0.2\ \mu\text{m}$. The agreements for the upper part of both nucleate boiling and transition boiling and the critical heat flux are quite satisfactory. At higher wall superheats, the model underpredicts the transition boiling heat flux. It is speculated that the barrier could be much thicker and that other deposits could be present. A barrier thickness of $1\ \mu\text{m}$, which is not impossible for a non-porous barrier [19], would have been sufficient to reduce the deviation between model predictions and experimental measurements significantly. The model prediction in contact-time fraction is also lower than the experimental measurement (in terms of contact-area fraction).

4. CONCLUSIONS

A theoretical model of transition boiling has been implemented by including transient conduction, boiling initiation, macrolayer evaporation and vapour film boiling. The model predictions agree reasonably well with experimental data, and the model is able to predict both of the transitions in boiling curve—the critical heat flux and minimum film boiling points. Evaluation of the model leads to the following conclusions.

(1) The inherent liquid turbulence is an important parameter in transition boiling and is predictable by a simple mixing theory incorporating buoyancy force and bubble agitation.

(2) Wall temperature drop at the end of the transient conduction period increases approximately linearly with increasing wall temperature before liquid contact.

(3) Liquid contact duration and contact-time fraction decrease very rapidly with increasing wall superheat.

(4) Surface coatings (oxidation or deposition) have very significant effects on transition boiling and cannot be neglected.

(5) The improvement of transition boiling due to the presence of a thin surface oxidation or deposition

may be explained, at least partially, by the oxide or deposit having poorer thermal properties than the heater material. In the literature, these effects were attributed to the improved wettability due to surface oxidation or deposition.

(6) The model predictions indicate that the presence of a thin insulating layer significantly increases the wall superheats at both the critical heat flux and the minimum film boiling points.

Although the current model is developed specifically for pool boiling, it is believed that the same concept can also be applied to transition boiling under flow boiling conditions; this is currently under study.

Acknowledgements—The authors would like to express their appreciation to Prof. Y. Y. Hsu for his critical review of the revised manuscript. This study was sponsored by National Science Council under contract numbers NSC-76-0413-E007-13 and NSC-77-0413-E007-13.

REFERENCES

1. L. Y. W. Lee, J. C. Chen and R. A. Nelson, Liquid–solid contact measurements using a surface thermocouple temperature probe in atmospheric pool boiling water, *Int. J. Heat Mass Transfer* **28**, 1415–1423 (1985).
2. L. C. Witte and J. H. Lienhard, On the existence of two-transition boiling curves, *Int. J. Heat Mass Transfer* **25**, 771–779 (1982).
3. Shin-Pin Liaw and V. K. Dhir, Effect of surface wettability on transition boiling heat transfer from a vertical surface, *Proc. 8th Int. Heat Transfer Conf.*, San Francisco, California, pp. 2031–2036. (1986).
4. P. J. Berenson, Experiments on pool boiling heat transfer, *Int. J. Heat Mass Transfer* **5**, 985–999 (1962).
5. J. W. Westwater and J. G. Santangelo, Photographic study of boiling, *I & EC Fundam.* **47**, 1605–1610 (1955). Paper reviewed in ref. [1].
6. B. J. Stock, Observations on transition boiling heat transfer phenomena, ANL-6175 (1960). Paper reviewed in ref. [1].
7. S. K. Roy Chowdhury and R. H. S. Winterton, Surface effects in pool boiling, *Int. J. Heat Mass Transfer* **28**, 1881–1889 (1985).
8. T. D. Bui and V. K. Dhir, Transition boiling heat transfer on a vertical surface, *J. Heat Transfer* **107**, 756–763 (1985).
9. Y. Kikuchi, T. Hori and I. Michiyoshi, The effect of thin insulating layer on heat transfer characteristics during quenching of hot metals in saturated water, *Trans. ISIJ* **26**, 576–581 (1986).
10. S. G. Bankoff and V. S. Mehra, A quenching theory for transition boiling, *I & EC Fundam.* **1**, 38–40 (1962). Paper reviewed in ref. [1].
11. Y. Katto and S. Yokoya, Principal mechanism of boiling crisis in pool boiling, *Int. J. Heat Mass Transfer* **11**, 993–1002 (1968).
12. R. F. Gaertner and J. W. Westwater, Population of active sites in nucleate boiling heat transfer, *Chem. Engng Prog. Symp. Ser.* **46**(30), 39–48 (1960).
13. R. F. Gaertner, Photographic study of nucleate pool boiling on a horizontal surface, *J. Heat Transfer* **87**, 17–29 (1965).
14. V. V. Kostyuk, I. I. Berlin and A. V. Karpyshev, Experimental and theoretical study of the transient boiling mechanism, *J. Engng Phys.* **50**, 38–45 (1986).
15. M. T. Farmer, B. G. Jones and B. W. Spencer, Analysis of transient contacting in the low temperature film boiling regime. Part I. Modeling of the process. Paper presented at 24th Natl Heat Transfer Conf., Pittsburgh, Pennsylvania, August (1987).
16. M. T. Farmer, B. G. Jones and B. W. Spencer, Analysis of transient contacting in the low temperature film boiling regime. Part II. Comparison with experiment. Paper presented at 24th Natl Heat Transfer Conf., Pittsburgh, Pennsylvania, August (1987).
17. Y. Y. Hsu and E. S. Kim, Transition boiling, *Int. Commun. Heat Mass Transfer* **15**, 533–558 (1988).
18. Y. Haramura and Y. Katto, A new hydrodynamic model of critical heat flux, applicable widely to both pool and forced convection boiling on submerged bodies in saturated liquids, *Int. J. Heat Mass Transfer* **26**, 389–399 (1983).
19. D. S. Dhuga and R. H. S. Winterton, Measurement of surface contact in transition boiling, *Int. J. Heat Mass Transfer* **28**, 1869–1880 (1985).
20. J. Y. Hwang, The mechanism of heat transfer in transition boiling, M. S. thesis, Department of Nuclear Engineering, National Tsing Hua University, Hsinchu, Taiwan, R.O.C. (1988), in Chinese.
21. P. J. Berenson, Film-boiling heat transfer from a horizontal surface, *J. Heat Transfer* **83**(3), 351–358 (1961).
22. Y. Y. Hsu, On the size range of active nucleation cavities on a heating surface, *J. Heat Transfer* **84**, 207 (1962).
23. R. Moissis and P. J. Berenson, On the hydrodynamic transition in nucleate boiling, *J. Heat Transfer* **85**, 221–229 (1963).
24. K. Nishikawa, T. Fujii and A. Honda, Experimental study on the mechanism of transition boiling heat transfer, *Bull. JSME* **15**, 93–103 (1972).
25. C.-L. Yu and R. B. Mesler, A study of nucleate boiling near the peak heat flux through measurement of transient surface temperature, *Int. J. Heat Mass Transfer* **20**, 827–840 (1977).
26. R. Mesler, Nucleate boiling in thin liquid films. In *Boiling Phenomena* (Edited by S. Van Stralen and R. Cole), Chap. 23. Hemisphere, Washington, DC (1979).
27. J. F. Davidson and B. O. G. Schueler, Bubble formation at an orifice in an inviscid liquid, *Trans. Inst. Chem. Engrs* **38**, 335–342 (1960). Paper reviewed in ref. [18].
28. J. K. Walters and J. F. Davidson, The initial motion of a gas bubble formed in an inviscid liquid. Part 2. The three dimensional bubble and the toroidal bubble, *J. Fluid Mech.* **17**, 321–336 (1963). Paper reviewed in ref. [18].
29. J. H. Lienhard, *A Heat Transfer Textbook*, Chap. 10. Prentice-Hall, Englewood Cliffs, New Jersey (1981).
30. C. M. Bender and S. A. Orszag, *Advanced Mathematical Methods for Scientists and Engineers*, Chap. 6. McGraw-Hill, New York (1978).
31. T. Aoki and J. R. Welty, Energy transfer mechanisms in transition pool boiling, *Int. J. Heat Mass Transfer* **13**, 1237–1240 (1970).
32. N. Zuber, On the stability of boiling heat transfer, *Trans. ASME* **80**, 711–720 (1958).
33. D. Y. T. Lin and J. W. Westwater, Effects of metal thermal properties on boiling curves obtained by the quenching method, *Proc. 7th Int. Heat Transfer Conf.*, Munich, Germany, Vol. 4, pp. 155–160 (1982).
34. M. E. Irving and J. W. Westwater, Limitations for obtaining boiling curves by the quenching method with spheres, *Proc. 8th Int. Heat Transfer Conf.*, San Francisco, California, Vol. 4, pp. 2061–2066 (1986).

LE MECANISME DE TRANSFERT DE CHALEUR DANS L'EBULLITION DE TRANSITION

Résumé—Le contact liquide–solide pendant l'ébullition de transition est modélisé en considérant la conduction variable, la naissance de l'ébullition, l'évaporation en macro-couche et l'ébullition avec film de vapeur. La prédiction de la durée du contact liquide et de la fraction de temps s'accorde raisonnablement bien avec des données expérimentales, et le modèle est capable de prédire les transitions de la courbe d'ébullition, les flux de chaleur critique et minimal. L'étude conclut que la turbulence du liquide due aux forces de flottement et à l'agitation des bulles est un paramètre important pour l'ébullition de transition. On trouve que le revêtement de surface (oxydation ou dépôt) tend à augmenter le transfert de chaleur et à élever les surchauffes de la paroi à la fois pour le flux critique et pour le flux minimal, ce qui s'accorde avec les observations expérimentales.

DER MECHANISMUS DES WÄRMEÜBERGANGS BEIM SIEDEN IM ÜBERGANGSGEBIET ZWISCHEN BLASEN- UND FILMVERDAMPFUNG

Zusammenfassung—Der Kontakt zwischen Flüssigkeit und fester Wand beim Sieden im Übergangsbereich zwischen Blasen- und Filmverdampfung wird unter Berücksichtigung der instationären Wärmeleitung, des Siedebeginns, der Verdampfung der Makroschichten und der Filmverdampfung modelliert. Die Berechnung der Kontaktdauer der Flüssigkeit an der Oberfläche und des entsprechenden Zeitanteils stimmt einigermaßen gut mit den experimentellen Werten überein. Das Modell kann sowohl die kritische als auch die minimale Wärmestromdichte berechnen. Die Untersuchung zeigt, daß die Flüssigkeitsturbulenz aufgrund von Auftriebskräften und von Blasenbewegungen ein wichtiger Parameter beim Übergangssieden ist. Es wurde festgestellt, daß die Beschichtung der Oberfläche (Oxidation oder Ablagerung) den Wärmeübergang beim Übergangssieden verbessert und die Wandüberhitzungen bei der kritischen Wärmestromdichte sowie beim Minimum des Filmsiedens erhöht. Dieses stimmt mit den experimentellen Beobachtungen überein.

МЕХАНИЗМ ТЕПЛОПЕРЕНОСА ПРИ КИПЕНИИ В ПЕРЕХОДНОМ РЕЖИМЕ

Аннотация—Исходя из нестационарного процесса теплопроводности, зарождения кипения, испарения макрослоя и кипения паровой пленки моделируется контакт жидкости с твердым телом при кипении в переходном режиме. Рассчитанная длительность контакта жидкости хорошо согласуется с экспериментальными данными. Модель позволяет также определить критический и минимальный тепловые потоки. Сделан вывод о том, что вызванная подъемными силами и перемешиванием пузырьков турбулентность является важным фактором при кипении в переходном режиме. Найдено, что при окислении поверхности или появлении отложений усиливается теплоперенос в процессе переходного кипения и повышается перегрев стенки как при критическом тепловом потоке, так и при минимальном пленочном кипении, что согласуется с экспериментальными наблюдениями.